

Numerical Optimization of Turboelectric Distributed Propulsion System in Hybrid Wing Body

A.Usha Bharathi
(ASST.PROFESSOR)

Department of aeronautical engineering,
Jeppiaar engineering college,
Chennai, India.

A. Hemalatha
(UG SCHOLAR),

Department of aeronautical engineering,
Jeppiaar engineering college,
Chennai, India.

S. Karthika
(UG SCHOLAR)

Department of aeronautical engineering,
Jeppiaar engineering college,
Chennai, India

Abstract - NASA N3-X Hybrid wing body aircraft has analysed for optimization of turboelectric distributed propulsion system mounted over aft portion of the fuselage. Here the aircraft configuration has increased strength and reduced weight. The CATIA model of N3-X has designed with 8, 12 and 16 propeller over the fuselage. The 3D meshing of aircraft meshed in hypermesh and simulation of different propeller configuration of N3-X is analysed in CFD-Fluent software. The turboelectric distributed propellers are evaluated with rotating wall boundary condition.

Keywords Propellers, Thrust, Turbulence, Pressure, velocity

I INTRODUCTION

The hybrid wing body also known as Blended wing body is a fixed-wing aircraft concept with zero clear separating line between the wing and main body of the aircraft. The wing and body structures of the aircraft are effortlessly blended together. These kinds of aircrafts have no distinct fuselage. This design aircraft may or may not be tailless. The main advantage of the aircraft is to produce greater lift and to reduce drag. It may be a wide aerofoil shaped body allowing the aircraft to produce greater lift which in reduces size and drag of the wing. The concept of HWB was initially developed and proposed by NASA in the early 1920. Studies shows that it could carry passengers of about 450 to 800. The HWB also have an advantage of less weight, less noise and emissions.

II PARAMETRIC MODELLING & MESHING PROCESSES

Several steps were done for modeling and meshing of a hybrid wing body. In first step, the designing of model with certain parameters are done. Fig 1 shows the HWB is designed with different number of propellers (8, 12 & 16) placing on aft position of the aircraft fuselage with a noise shield covering in it. The propeller is designed with three rotating shafts with a connector and base. The second step includes meshing of aircraft by tetrahedral meshing methods with necessary element sizes is shown in fig covering in it. The propeller is designed with three rotating shafts with a connector and base. The second step includes meshing of aircraft by tetrahedral meshing methods with necessary element sizes is shown in fig.

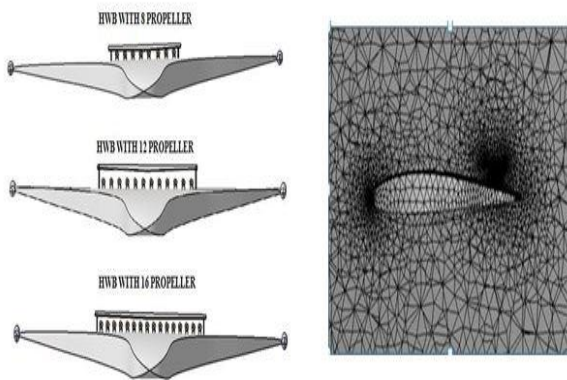


Fig 1 Design & meshing of HWB

III FLOW VISUALIZATION OF HWB

The flow domain over the Hybrid Wing Body with propeller is taken in such a way so that the stream of air flows freely around the nook and corner of the propeller.

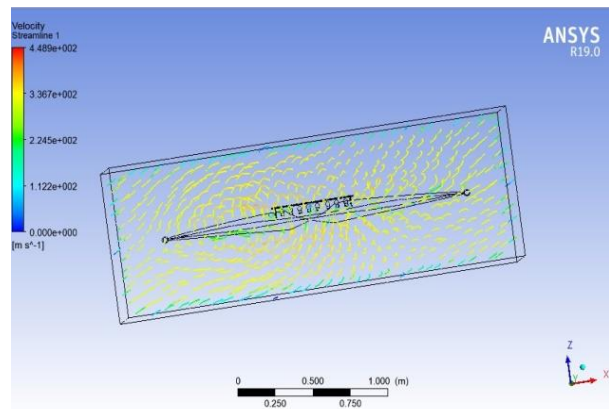


Fig 2 Flow visualization of HWB

The figure shows the streamline flow of velocity of Hybrid Wing Body with Propeller.

The figure clearly shows when flow arising from inlet reaches the propeller interact the flow coming from the rotating propeller thus making the flow diverted around the propeller.

IV BOUNDARY CONDITION AND SOLVER SETTING

Table 1 .Boundary condition & solver settings

TYPE	DESCRIPTION
Solver	Pressure based Navier stoke's equation
Flow	Transient
Fluid	Ideal gas
Inlet	Velocity(285.6,251.6, 319.6m/s)
Outlet	Pressure 0 Pa
Moving wall	4500 RPM

V COMPUTATIONAL RESULTS AND DISCUSSION

NAVIER-STOKES EQUATIONS:

Continuity Equation:

$$\frac{\partial \rho}{\partial t} + \frac{\partial(\rho u)}{\partial x} + \frac{\partial(\rho v)}{\partial y} + \frac{\partial(\rho w)}{\partial z} = 0$$

Momentum Equation:

In X – Direction

$$\frac{\partial(\rho u)}{\partial t} + \frac{\partial(\rho u^2)}{\partial x} + \frac{\partial(\rho uv)}{\partial y} + \frac{\partial(\rho uw)}{\partial z} = - \frac{\partial p}{\partial x} + \frac{1}{Re_{\tau}} \left[\frac{\partial \tau_{xx}}{\partial x} + \frac{\partial \tau_{xy}}{\partial y} + \frac{\partial \tau_{xz}}{\partial z} \right]$$

In Y – Direction

$$\frac{\partial(\rho v)}{\partial t} + \frac{\partial(\rho uv)}{\partial x} + \frac{\partial(\rho v^2)}{\partial y} + \frac{\partial(\rho vw)}{\partial z} = - \frac{\partial p}{\partial y} + \frac{1}{Re_{\tau}} \left[\frac{\partial \tau_{xy}}{\partial x} + \frac{\partial \tau_{yy}}{\partial y} + \frac{\partial \tau_{yz}}{\partial z} \right]$$

In Z – Direction

$$\frac{\partial(\rho w)}{\partial t} + \frac{\partial(\rho uw)}{\partial x} + \frac{\partial(\rho vw)}{\partial y} + \frac{\partial(\rho w^2)}{\partial z} = - \frac{\partial p}{\partial z} + \frac{1}{Re_{\tau}} \left[\frac{\partial \tau_{xz}}{\partial x} + \frac{\partial \tau_{yz}}{\partial y} + \frac{\partial \tau_{zz}}{\partial z} \right]$$

Energy Equation:

$$\begin{aligned} \frac{\partial(E_t)}{\partial t} + \frac{\partial(uE_t)}{\partial x} + \frac{\partial(vE_t)}{\partial y} + \frac{\partial(wE_t)}{\partial z} = - \frac{\partial(pu)}{\partial x} - \frac{\partial(pv)}{\partial y} - \frac{\partial(pw)}{\partial z} - \\ \frac{1}{Re_{\tau} Pr_{\tau}} \left[\frac{\partial q_x}{\partial x} + \frac{\partial q_y}{\partial y} + \frac{\partial q_z}{\partial z} \right] + \frac{1}{Re_{\tau}} \left[\frac{\partial}{\partial x} (u\tau_{xx} + v\tau_{xy} + w\tau_{xz}) + \frac{\partial}{\partial y} (u\tau_{xy} + v\tau_{yy} + w\tau_{yz}) + \frac{\partial}{\partial z} (u\tau_{xz} + v\tau_{yz} + w\tau_{zz}) \right] \end{aligned}$$

A. Pressure contour at 0.74 mach no

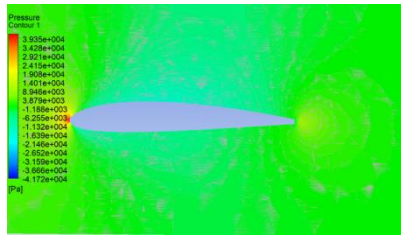


Fig 3 Without propeller

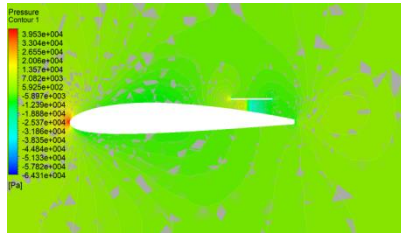


Fig 4 With 8 propeller

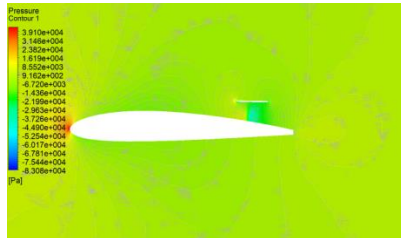


Fig 5 With 12 propeller

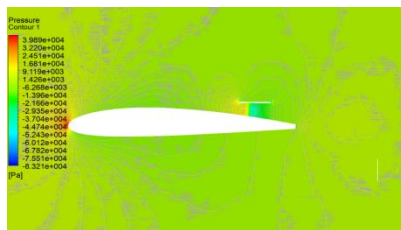


Fig 6 With 16 propeller

The figure shows the analysis of pressure contour for HWB with and without propeller at different mach number. From the figure, it is seen that HWB at all mach number have low pressure above the aircraft and high pressure below the aircraft which produces greater lift to fly. The total pressure produced for HWB without propeller at 0.74 mach no is 20657.3 Pa and for 8, 12 & 16 propeller is 18324.19, 17891.02 & 17998.31 Pa. The total pressure produced for HWB without propeller at 0.84 mach no is

26668.51 Pa and for 8, 12 & 16 propellers is 23699.6, 23252.83 & 23202.84 Pa.

The total pressure produced for HWB without propeller at 0.94 mach no is 33446.56 Pa and for 8, 12 & 16 propeller is 29653.1, 29251.2 & 29201.88 Pa.

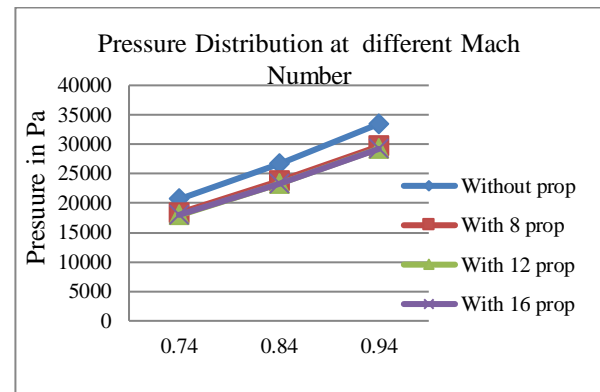


Fig 7 Pressure distribution

By observation the aircraft with 16 propellers at 0.74 mach number produces lesser pressure (approximately 13 %) compared to aircraft without propeller and with 8 and 12 propellers

B. Velocity contour at 0.74 mach no

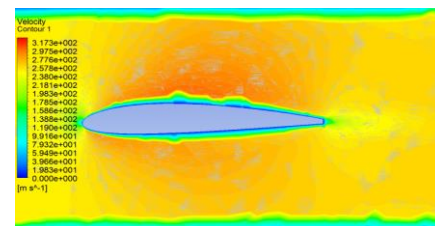


Fig 8 Without propeller

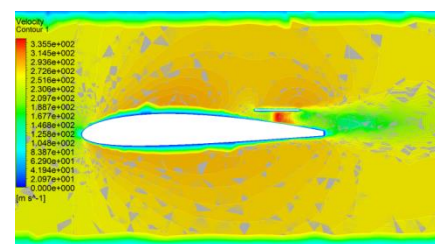


Fig 9 With 8 propeller

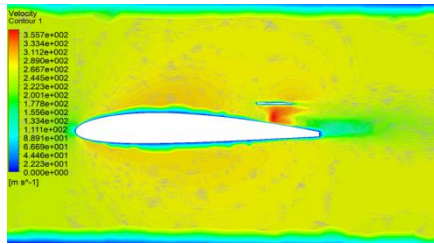


Fig 10 With 12 propeller

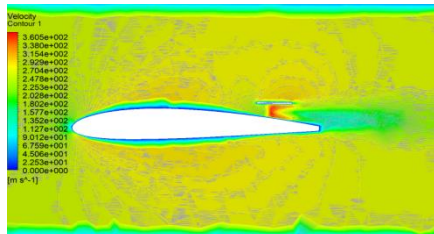


Fig 11 With 16 propeller

The above figure shows the analysis of velocity contour for HWB with and without propeller at different Mach number. From the figure, it is seen that the Velocity is high above the aircraft and low below the aircraft. The minimum amount of velocity is created at the cockpit of HWB. The combination of interacted propeller velocity and remaining velocity moves in between the gap of propeller and creates a greater velocity at backward portion of propeller.

The maximum velocity produced for HWB without propeller at 0.74 Mach number is 297.5 m/s and for 8, 12 & 16 propeller is 335.7, 355.7 & 360.5 m/s.

The maximum velocity produced for HWB without propeller at 0.84 Mach number is 337.6 m/s and for 8, 12 & 16 propeller is 380.9, 403.6 & 409.2 m/s.

The maximum velocity produced for HWB without propeller at 0.94 Mach number is 377.9 m/s and for 8, 12 & 16 propeller is 435.3, 451.5 & 458 m/s.

From the graph we can see that the velocity continuously increases when number of propeller increases and these velocity continuously increases up to certain Mach number.

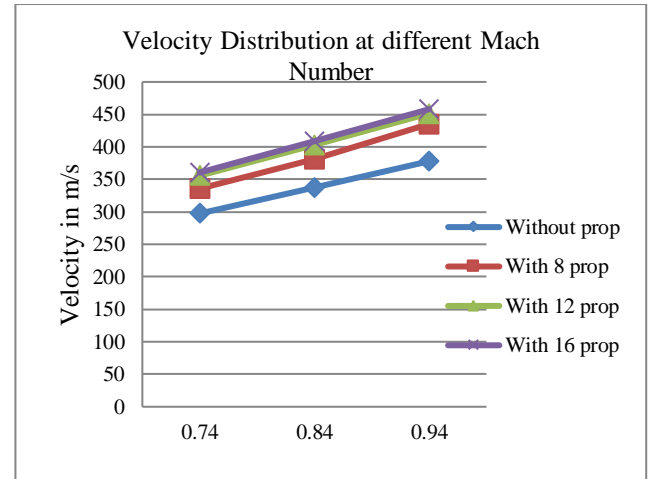


Fig 12 Velocity distribution

By observation, the velocity for aircraft with 16 propeller at 0.74 mach no increases of about 21% approximately when compared to other cases of the aircraft with 8 & 12 propellers and for without propeller.

C. Turbulence contour at 0.74 mach no

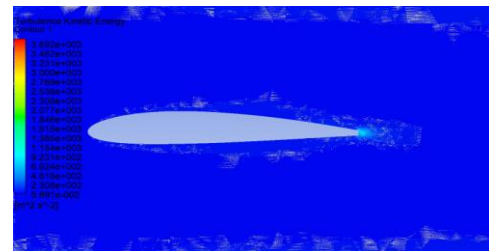


Fig 13 Without propeller

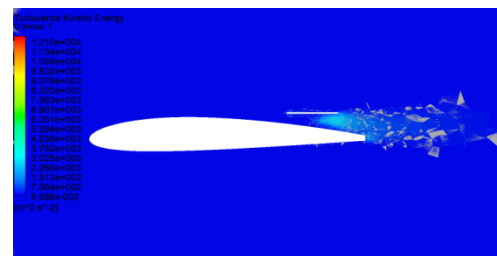


Fig 14 With 8 propeller

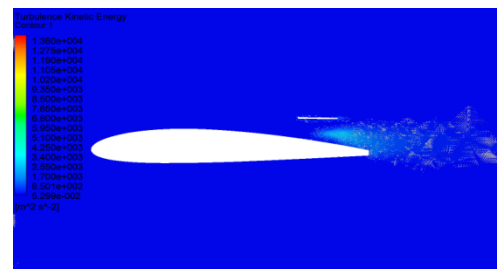


Fig 15 With 12 propeller

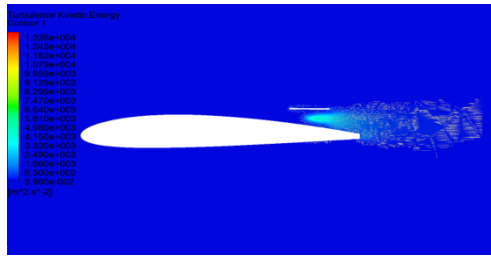


Fig 16. With 16 propeller

From the figure, it can be seen that no turbulent kinetic energy is formed from cockpit to aft position of fuselage.

The maximum amount of turbulence produced for HWB without propeller at 0.74 mach number is $133.3 \text{ m}^2/\text{s}^2$ and for 8, 12 & 16 propeller is 224.46, 272.31 & $293.35 \text{ m}^2/\text{s}^2$.

The maximum amount of turbulence produced for HWB without propeller at 0.84 Mach number is $168.9 \text{ m}^2/\text{s}^2$ and for 8, 12 & 16 propeller is 285.91, 348.78 & $375.38 \text{ m}^2/\text{s}^2$.

The maximum amount of turbulence produced for HWB without propeller is $208.6 \text{ m}^2/\text{s}^2$ and for 8, 12 & 16 propeller is 355.32, 433.6 & $466.35 \text{ m}^2/\text{s}^2$.

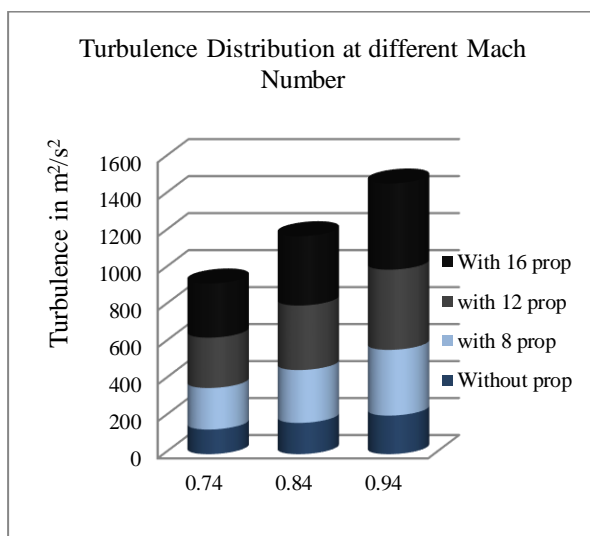


Fig 17 Turbulence distribution

From the turbulence distribution chart, we can conclude that the turbulence are produced when propeller are placed in HWB.

Hence, the amount of turbulence increases when number of propeller increases.

Compared to other cases, the aircraft with 16 propellers at 0.74 mach no produces lesser turbulence of about 120%.

VI THRUST DEVELOPED FOR VARIOUS CASES OF HWB

Table 2 Thrust development

Various cases of HWB	Thrust developed in N
Without propeller at 0.74 mach no	3844.33
With 8 propeller at 0.74 mach no	4392.42
With 12 propeller at 0.74 mach no	4535.16
With 16 propeller at 0.74 mach no	4902.77
Without propeller at 0.84 mach no	4949.91
With 8 propeller at 0.84 mach no	5654.06
With 12 propeller at 0.84 mach no	6018.89
With 16 propeller at 0.84 mach no	6314.88
Without propeller at 0.94 mach no	6195.32
With 8 propeller at 0.94 mach no	7072.09
With 12 propeller at 0.94 mach no	7528.03
With 16 propeller at 0.94 mach no	7902.6

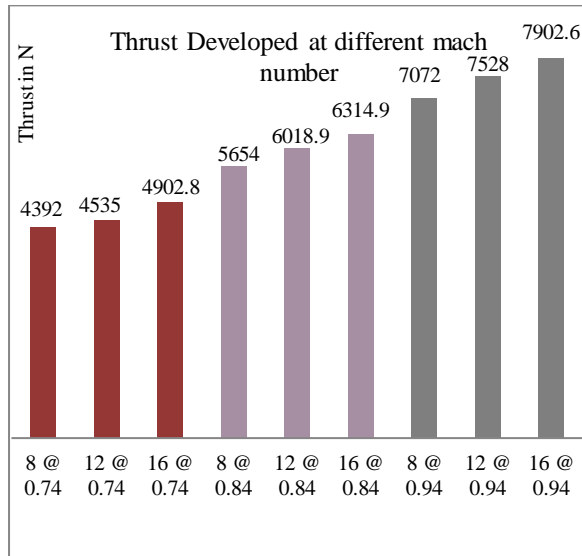


Fig 18 Thrust increment

From the figure and the table, it can be seen that thrust for HWB with 8, 12 & 16 propeller at 0.74 Mach number are increases gradually when number of propeller increases.

We can conclude that thrust continuously increases when number of propeller increases.

VII CONCLUSION

Thrust is the necessary force which moves an aircraft through the air. The greater thrust and lesser turbulence will give a better aircraft performance. From the analysis, we observed that the Hybrid Wing Body with 16 propellers produces greater thrust when compared to Hybrid Wing Body with 8 and 12 propellers. From the table, we can conclude that the amount of Thrust improvement is almost similar at 0.74, 0.84 and 0.94 Mach number. Therefore by choosing Hybrid Wing Body with 16 propellers at 0.74 Mach number, we can get a better aircraft configuration. This is because of greater thrust production improvement up to 21.58% and lesser turbulence when compared with other 2 Mach number.

Hence the HWB with 16 propellers at 0.74 Mach number can produce greater Thrust

to overcome drag and lesser Turbulence will provide better safety for an aircraft from damage.

IX REFERENCES

- [1] NASA Research and Technology Program and Project Management Requirements, NASA Procedural Requirements 7120.9. Appendix J. Technology Readiness Levels (TRLs), February 05, 2008
- [2] Greitzer, Edward M., et al, "N3 Aircraft Concept Designs and Trade Studies," NASA Contractor Report CR-2010-216794, Volume 1 and 2, 2010
- [3] Bruner, Sam, et al., "NASA N3 Subsonic Fixed Wing Silent Efficient Low-Emissions Commercial Transport (SELECT) Vehicle Study," NASA Contractor Report CR-2010-216798, 2010
- [4] Bradley, M. and Droney, C, "Subsonic Ultra Green Aircraft Research: Phase I Final Report", NASA Contract Number NNL08AA16B, 2010
- [5] Liebeck, R., "Design of the Blended Wing Body Subsonic Transport", *Journal of Aircraft*, Vol. 41, No. 1, Jan-Feb. 2004. pp. 10-25
- [6] Thomas.R, Burley, C., Olson, E., "Hybrid Wing Body Aircraft System Noise Assessment with Propulsion Airframe Aeroacoustic Experiments", AIAA-2010-3913, 2010.
- [7] Tillman, Greg, et all, "Robust Design for Embedded Engine Systems – BLI Inlet and Distortion-Tolerant Fan Design", NASA Contract Number NNC07CB59C, 2010
- [8] "Lightweight, Efficient Power Converters for Advanced Turboelectric Aircraft Propulsion Systems", Final Report, NASA 2010 Phase 1 SBIR,

NNX10CC71P, MTECH Laboratories, LLC, July 29, 2010.

[9] Gohardani, A. S., Doulgeris, G. and Singh, R. (2011), "Challenges of future aircraft propulsion: A review of distributed propulsion technology and its potential application for the all-electric commercial aircraft",

[10] Kawai, R., Brown, D., Roman, D. and Olde, R. (Oct. 2008), "Acoustic Prediction Methodology and Test Validation for an Efficient Low-noise Hybrid Wing Body"

[11] Brown, G. V. (2011), Weights and Efficiencies of Electric Components of a Turboelectric Aircraft Propulsion System.

[12] Costi, F. (2012), "Investigation on boundary layer ingestion effects on a ducted axial fan for distributed propulsion system"

WEBSITE

www.nasaeaglework.com.

www.wikipedia.org

www.Airfoil Database Investigation.com